Mon. Not. R. Astron. Soc. **000**, 000–000 (0000) Printed 3 March 2024 (MN LATEX style file v2.2)

# Abundance Anomalies In Tidal Disruption Events

C. S. Kochanek[1,2]
[1] *Department of Astronomy, The Ohio State University, 140 West 18th Avenue, Columbus OH 43210*
[2] *Center for Cosmology and AstroParticle Physics, The Ohio State University, 191 W. Woodruff Avenue, Columbus OH 43210*

3 March 2024

arXiv:1512.03065v1 [astro-ph.HE] 9 Dec 2015

**ABSTRACT**
The $\sim 10\%$ of tidal disruption events (TDEs) due to stars more massive than $M_* \gtrsim M_\odot$ should show abundance anomalies due to stellar evolution in helium, carbon and nitrogen, but not oxygen. Helium is always enhanced, but only by up to $\sim 25\%$ on average because it becomes inaccessible once it is sequestered in the high density core as the star leaves the main sequence. However, portions of the debris associated with the disrupted core of a main sequence star can be enhanced in helium by factors of 2-3 for debris at a common orbital period. These helium abundance variations may be a contributor to the observed diversity of hydrogen and helium line strengths in TDEs. A still more striking anomaly is the rapid enhancement of nitrogen and the depletion of carbon due to the CNO cycle – stars with $M_* \gtrsim M_\odot$ quickly show an increase in their average $N/C$ ratio by factors of 3-10. Because low mass stars evolve slowly and high mass stars are rare, TDEs showing high $N/C$ will almost all be due to 1-2$M_\odot$ stars disrupted on the main sequence. Like helium, portions of the debris will show still larger changes in C and N, and the anomalies decline as the star leaves the main sequence. The enhanced $[N/C]$ abundance ratio of these TDEs provides the first natural explanation for the rare, nitrogen rich quasars and also explains the strong nitrogen emission seen in ultraviolet spectra of ASASSN-14li.

**Key words:** stars: black holes

## 1 INTRODUCTION

If a star passes too close to a supermassive black hole, it can be completely or partially destroyed by tides. Portions of the debris are then accreted by the black hole, leading to a luminous tidal disruption event (TDE, e.g., Lacy et al. 1982, Rees 1988, Evans & Kochanek 1989). Arcavi et al. (2014) noted that TDEs show a remarkable diversity in the relative strengths of the hydrogen H$\alpha$/H$\beta$ Balmer lines and the HeII 4686Å emission line. In the most extreme cases, the broad HeII emission lines are significantly stronger than the Balmer lines (PS1-10jh, Gezari et al. (2012); PTF09ge, Kasliwal et al. (2009), ASASSN-15oi REF), while others show both strong HeII and Balmer emission lines (SDSS J074820.66+471214.6, Wang et al. (2012); ASASSN-14ae, Holoien et al. (2014); ASASSN-14li, Holoien et al. (2016)). There are also some that appear hydrogen dominated (PTF09djl, PTF09axc, Arcavi et al. (2014); TDE2, van Velzen et al. (2011), and possibly PS1-11af, Chornock et al. (2014)). This is quite curious because in typical AGN and quasars the HeII 4686Å emission line is generally very weak compared to H$\alpha$ and H$\beta$ (e.g. Vanden Berk et al. 2001).

Debates over the origin of strong HeII emission in TDEs have mainly focused on PS10jh, where Gezari et al. (2012) proposed that the spectrum, with strong HeII 4686Å and undetected H Balmer emission ($\gtrsim$ 5:1 ratio), could only be explained by disrupting a helium star. Guillochon et al. (2014), based on the quasar broad line region models of Korista & Goad (2004), argued that there were parameter ranges that could almost reproduce the observed line ratios at Solar abundance. Their physical explanation for the origin of the strong helium emission ("matter bounding" a quasar broad line region to include only the inner, higher ionization line regions) is not, however, correct. As explained in Gaskell & Rojas Lobos (2014), the key at Solar metallicity lies in finding a density regime where line opacities can drive the line ratios close to the thermal limit where the HeII 4686Å line is $(6563/4686)^4 = 3.8$ times stronger than H$\alpha$.

Strubbe & Murray (2015) broadly argue that the underlying `CLOUDY` models used by Guillochon et al. (2014) and Gaskell & Rojas Lobos (2014) are inapplicable to the TDE problem. First, they argue that the AGN-like spectra do not match the observed spectral energy distributions of TDEs. It is certainly true that some optical/UV TDEs have weak or undetected X-ray emission, but others have X-ray emission indicating the existence of a hard tail (e.g. Holoien et al. 2016). Second, they argue that an optically thin ionized medium cannot have a line ratio exceeding the volume emissivity ratio for a fully ionized $He^{++}$

© 0000 RAS

region, other than by changing the underlying abundances from Solar ($n(He)/n(H) \simeq 0.09$ for $X = 0.70$, $Y = 0.28$ and $Z = 0.02$). Third, they argue that the CLOUDY models used by Guillochon et al. (2014) and Gaskell & Rojas Lobos (2014) assume thermal line widths ($\sim$ 10 km/s), far smaller than the observed line widths ($> 10^3$ km/s). Hence, for the same physical parameters, the lines are far less optically thick than assumed by the CLOUDY models. Roth et al. (2015), however, find that extreme hydrogen to helium line ratios are achievable at Solar metallicity using broad line widths and radiation transfer models better suited to high optical depths than CLOUDY.

All these calculations have assumed that the debris has Solar composition. This may be true at birth on the zero age main sequence (ZAMS), but it becomes increasingly less so as the star evolves. In particular, the star becomes steadily more helium rich as it evolves. Hydrogen burning through the CNO cycle also modifies carbon, nitrogen and oxygen abundances, primarily by reducing the amount of carbon and increasing the amount of nitrogen. There are also changes in lithium and beryllium abundances and CNO isotope ratios, but these will not be observable in TDEs because of Doppler line broadening.

For a normal star, these internal changes have no external consequences until close to death, when convection on the giant branch can mix material from the hydrogen burning zone to the surface ("dredge up"). In a TDE, however, material processed by nuclear reactions is revealed without any need to wait for these late phases of stellar evolution, and some of the debris will have abundances and metallicities that are never observed in stellar atmospheres (other than Wolf-Rayet stars) or the interstellar medium. In §2 we examine the evolution of the helium and CNO abundances for stars with a range of masses and how this will manifest itself in a TDE. In §3 we discuss nitrogen rich quasars and suggest that they are likely the remnants of recent TDEs. We summarize the results and their observational implications in §4. In particular, we note that the ultraviolet spectrum by Cenko et al. (2015) of the TDE ASASSN-14li (Holoien et al. 2016) bears a striking similarity to spectra of nitrogen rich quasars.

## 2 ABUNDANCE ANOMALIES IN TDES

For our analyses we ran generic Solar metallicity ($X = 0.70$, $Y = 0.28$, $Z = 0.02$) MESA (Paxton et al. 2013) models. In Figures 1 to 3, we show the evolution of the helium, carbon and nitrogen abundances for $M_* = 0.5M_\odot$, $1M_\odot$ and $2M_\odot$ in three regions: the entire star, outside the inner edge of the hydrogen burning zone, and outside the outer edge of the hydrogen burning zone. The zone edges are defined by the radius where the hydrogen energy generation rate exceeds 1 erg g$^{-1}$ s$^{-1}$. These roughly represent the regions of the star that are likely to be disrupted. On the main sequence, typically the star will be completely disrupted (e.g. Evans & Kochanek 1989, Guillochon & Ramirez-Ruiz 2013). Evolved stars, however, are only likely to be stripped into the hydrogen burning zone because of the huge jump in density at its base. The stripping of the envelope may also require several pericentric passages rather than occurring a single event (MacLeod et al. 2012).

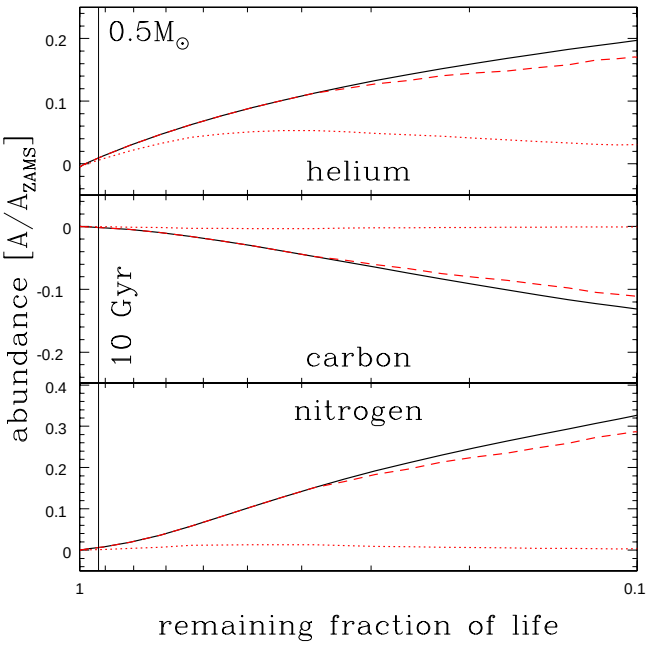



**Figure 1.** Change in abundance $[A(t)/A(0)]$ from that on the ZAMS for helium (top), carbon (middle) and nitrogen (bottom) as a function of the remaining fractional life time of a $0.5M_\odot$ star. The heavy solid curve is for the entire star and the red dashed (dotted) line is for the material outside the inner (outer) edge of the hydrogen burning region (defined by $\epsilon > 1$ erg g$^{-1}$ s$^{-1}$). Main sequence turn off occurs as the curve for the inner edge of the hydrogen burning region diverges from the results for the entire star. A vertical line marks an age of 10 Gyr. Low mass stars, like this $0.5M_\odot$ example, do not have time to develop abundance anomalies given the age of the universe.

Figure 1 shows that low mass stars simply live too long to develop abundance anomalies given the age of the universe. Over its main sequence life time, an $0.5M_\odot$ star becomes significantly enhanced in helium and nitrogen and depleted in carbon, but 10 Gyr represents less than 10% of its overall lifetime of $\sim$ 130 Gyr. Unlike more massive stars, the carbon and nitrogen anomalies grow slowly because the p-p chain dominates the fusion rates. *Producing an abundance anomaly in a TDE requires an* $\gtrsim 1M_\odot$ *star.*

Sun-like stars live $\simeq$ 12 Gyr, which means that they will be disrupted at a roughly random evolutionary phase for galaxies with a constant star formation rate and at a late evolutionary phase for galaxies dominated by early bursts of star formation. Figure 2 shows the average abundance evolution with age for a $1M_\odot$ star. The general evolution is the same until the late phases (note that Figure 2 covers 99% of the stellar lifetime rather than the 90% shown in Figure 1). On the main sequence, it develops a modest average enhancement of helium, a somewhat larger depletion of carbon, and a still larger enhancement of nitrogen. By the mid-point of its main sequence evolution, the $[N/C]$ abundance ratio has increased by a factor of three compared to its initial value, and as it leaves the main sequence, the enhancement is roughly a factor of four. While the p-p chain still dominates the overall fusion rate, CNO cycle reactions are sufficiently important to more rapidly alter the carbon

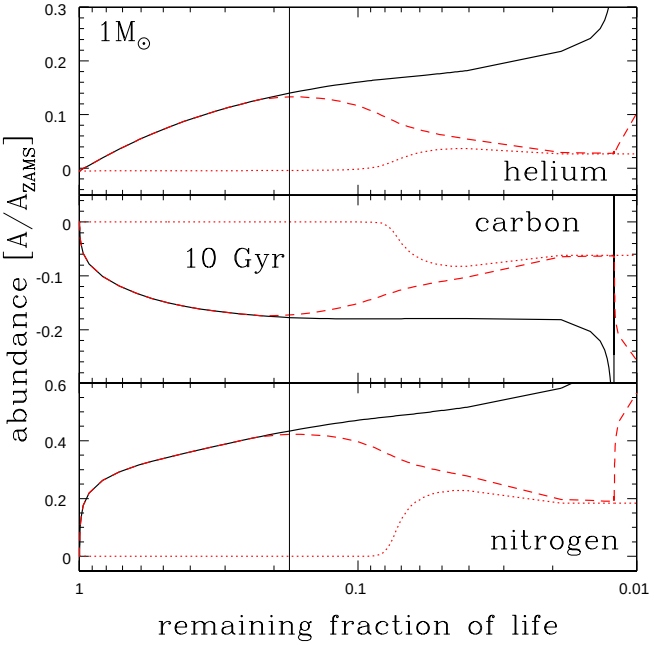



**Figure 2.** Change in abundance $[A(t)/A(0)]$ from that on the ZAMS for helium (top), carbon (middle) and nitrogen (bottom) as a function of the remaining fractional life time of a $1.0M_\odot$ star. The heavy solid curve is for the entire star and the red dashed (dotted) line is for the material outside the inner (outer) edge of the hydrogen burning region. A vertical line marks an age of 10 Gyr. For a constant star formation rate over the age of the universe, Sun-like stars will be disrupted at a roughly random evolutionary phase. For an old stellar population, Sun-like stars will be near or past the main sequence turnoff.

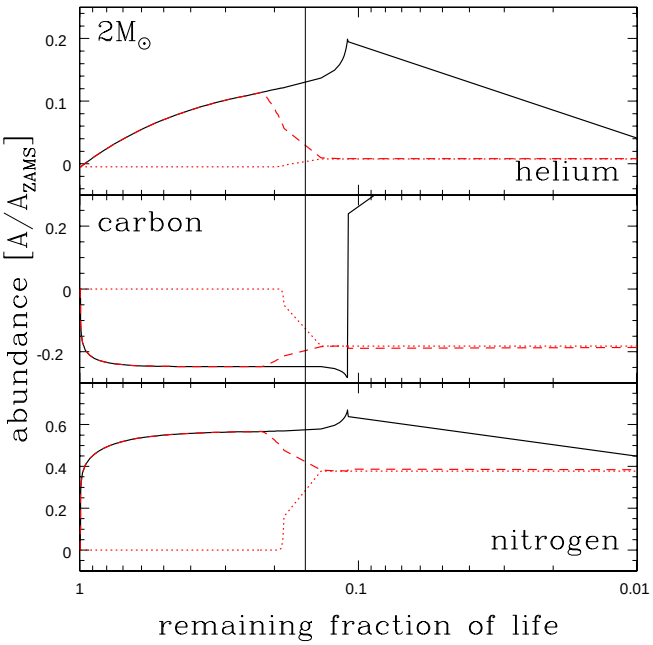



**Figure 3.** Change in abundance $[A(t)/A(0)]$ from that on the ZAMS for helium (top), carbon (middle) and nitrogen (bottom) as a function of the remaining fractional life time of a $2.0M_\odot$ star. The heavy solid curve is for the entire star and the red dashed (dotted) line is for the material outside the inner (outer) edge of the hydrogen burning region. A vertical line marks an age of 1 Gyr. For shorter lived massive stars, the evolutionary state at the time of disruption will become nearly random and independent of the star formation history.

and nitrogen abundances. During the MS evolution, the average oxygen abundance slowly drops, but only by $\sim 10\%$ of the carbon depletion. As the star begins hydrogen shell burning, the anomalies outside the helium core begin to drop again. However, first dredge up also mixes them into the outer parts of the star beyond the shell. Figure 2 extends a little past the horizontal branch, where we first see a rapid increase in helium followed by a rapid increase in carbon.

Figure 3 shows the results for a $2M_\odot$ star. The general pattern is similar to that for a $1M_\odot$ star except that the time scales are greatly accelerated since the life time of the star is now only 1.2 Gyr. The average helium abundance slowly rises, while there is a rapid average depletion of carbon and enhancement of nitrogen. Oxygen is again slightly depleted on the MS. Because the CNO cycle is much more important, the overall scale of the carbon and nitrogen anomalies is significantly larger. At the mid-point of its lifetime, the $[N/C]$ ratio is increased by a factor of 6 on average, and the abundance ratio continues to increase slowly until the star leaves the main sequence. First dredge up again mixes some of the processed material into the outer regions of the star. In the later evolutionary phases, the regions from the hydrogen burning shell outwards have little enhancement in helium and smaller changes in $[N/C]$. As stellar lifetimes become short compared to the typical time scales of star formation, the evolutionary phase at the time of disruption will be increasingly independent of the star formation history.

Figure 4 summarizes the behavior of $[N/C]$ anomalies with stellar mass. For stars with lifetimes $< 10$ Gyr ($M_* \lesssim M_\odot$), we show the change in abundance at 10 Gyr. For more massive, shorter lived stars, we show the peak increase in $[N/C]$ excluding the regions inside hydrogen burning shells (which generally means the values close to main sequence turn off). Lower mass stars have negligible increases in $[N/C]$ because the universe is too young and the p-p chain dominates the reaction rates, while higher mass stars can have nitrogen enhanced relative to carbon by an order of magnitude due to the increasing importance of the CNO cycle.

To make a rough estimate of the fraction of stars likely to show anomalies, we need a scaling of the disruption rate with stellar mass, a model for the IMF and a star formation history. If we follow Wang & Merritt (2004) or MacLeod et al. (2012), the TDE rate scales as $R_*^{1/4} M_*^{-1/12} \simeq M_*^{1/6}$ if we roughly scale $R_* \propto M_*$ for the MS. Higher mass stars have lower densities and so have higher rates. Stars closer to the main sequence turn off also have lower densities than on the ZAMS, but we make no attempt to include this effect. For the IMF we follow Kroupa (2001) with $(dn/dM_*)_{IMF} \propto (M_*/M_b)^{-x}$ with $x = -1.3$ for $0.08M_\odot < M_* < M_b = 0.5M_\odot$ and $x = -2.3$ for $M_* > M_b$. We show the rate per logarithmic interval of mass, $M_*(dr/dM_*)$, where the rate per unit mass, $dr/dM_*$, is proportional to the scaling of the TDE rate with stellar

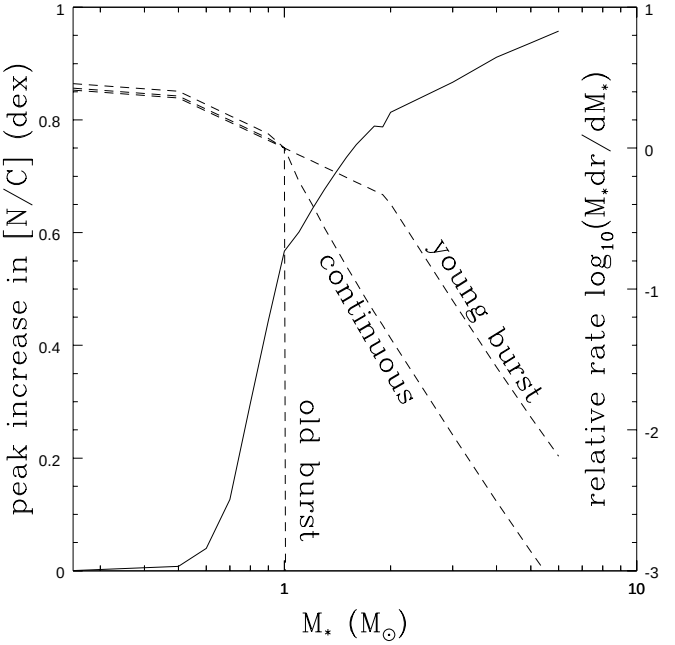



**Figure 4.** Peak enhancement in $[N/C]$ relative to the ZAMS abundance ratio (left scale, solid curve) as a function of stellar mass $M_*$ assuming a maximum stellar age of 10 Gyr. Low mass stars ($M_* \lesssim M_\odot$) have no time to develop $[N/C]$ anomalies given the age of the universe, while high mass stars quickly generate large anomalies as the CNO cycle becomes more important. The dashed curves (right scale) roughly show the scaling of TDE rates per logarithmic mass interval ($M_*(dr/dM_*)$) for an old star burst (2 Gyr of star formation 10 Gyr ago), continuous star formation, and a recent star burst (last 1 Gyr).

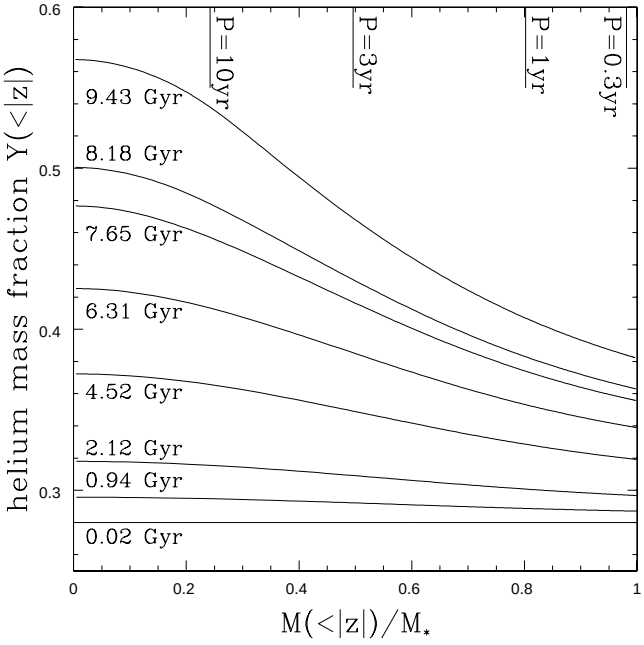



**Figure 5.** Enclosed helium mass fraction $Y(<|z|)$ as function of the enclosed mass fraction $M_*(<|z|)/M_*$ for a $M_* = 1M_\odot$ star. The coordinate $z$ is the distance from the center of the star towards the black hole at pericenter. Profiles are shown at the indicated times from 0.02 Gyr to core hydrogen exhaustion near 9.43 Gyr. Vertical bars show the orbital period assuming $M_{BH} = 10^6 M_\odot$ and a disruption at $R_p = R_*(M_{BH}/M_*)^{1/3}$ at roughly the age of the Sun.

mass, the IMF, and the number of stars available at the mass given the star formation history.

Figure 4 also shows the scaling of TDE rates with stellar mass given these assumptions and three possible star formation histories: an old burst of star formation, continuous star formation and a recent burst of star formation. The rates are all normalized by the rate at $M_* = M_\odot$. For an old stellar population ("old burst" in Figure 4) we assume 2 Gyr of constant star formation starting 10 Gyr in the past. For this model, the rate is proportional to the product of the IMF and the scaling of rates with stellar mass for stars with main sequence lifetimes less than $\sim 8$ Gyr followed by an abrupt cut off because main sequence lifetimes $t_{MS}(M_*)$ are such a steep function of mass. For $t_0 = 10$ Gyr of continuous star formation, the number of stars at a given mass scales as the IMF multiplied by $\min(t_0, t_{MS})$, which produces a less abrupt break near $M_* = M_\odot$. Finally, we show the relative rates for a recent 1 Gyr starburst ("young burst"). The combined effects of the dropping IMF and the rapid evolution of higher mass stars means that they contribute little to the rate of TDEs independent of the star formation history. The slow evolution of low mass stars mean that they contribute little to abundance anomalies. As a result, nitrogen rich, carbon poor TDEs should be sign posts for the disruption of 1-2$M_\odot$ stars. For these various assumptions, the rate of TDEs with $M_* \gtrsim M_\odot$ is of order 7% to 14% of the total rate. However, when the fraction is low, the stars will tend to be closer to the main sequence turn off where the abundance anomalies are large, and *vice versa* when the fraction is high. Hence, a reasonable order of magnitude estimate is that $\sim 10\%$ of TDEs will show strong abundance anomalies.

So far we have only examined the average abundances of the material likely to form the debris of a TDE. In practice, the processed material is highly stratified and concentrated towards the center with negligible changes outside the hydrogen burning regions until first dredge up on the red giant branch. The disruption process sorts the debris by orbital period (e.g. Rees 1988), where the period is basically determined by the distance of the material $z$ along the direction towards the black hole at pericenter. For a parabolic orbit, the binding energy of the debris is $-GM_{BH}z/R_p^2$, implying a semi-major axis of $a = R_p^2/2z$. If we disrupt at $R_p = R_T = R_*(M_{BH}/M_*)^{1/3}$, then the orbital period is

$$\begin{aligned} P &= \frac{\pi}{\sqrt{2}}\left(\frac{M_{BH}}{M_*}\right)^{1/2}\left(\frac{R_*}{z}\right)^{3/2}\left(\frac{R_*^3}{GM_*}\right)^{1/2} \\ &= 0.11\left(\frac{R_*}{z}\right)^{3/2} \text{ years} \end{aligned} \quad (1)$$

for Solar units and $M_{BH} = 10^6 M_\odot$. Hence, we next examine abundance anomalies as a function of $|z|$, corresponding to planar slices through the star from the slice through the center at $z = 0$ (with a nominally infinite period for a parabolic orbit) to a slice just grazing the surface at $|z| = R_*$. While the distribution in $|z|$ is symmetric, material with $z > 0$ is bound and can potentially be accreted, while material

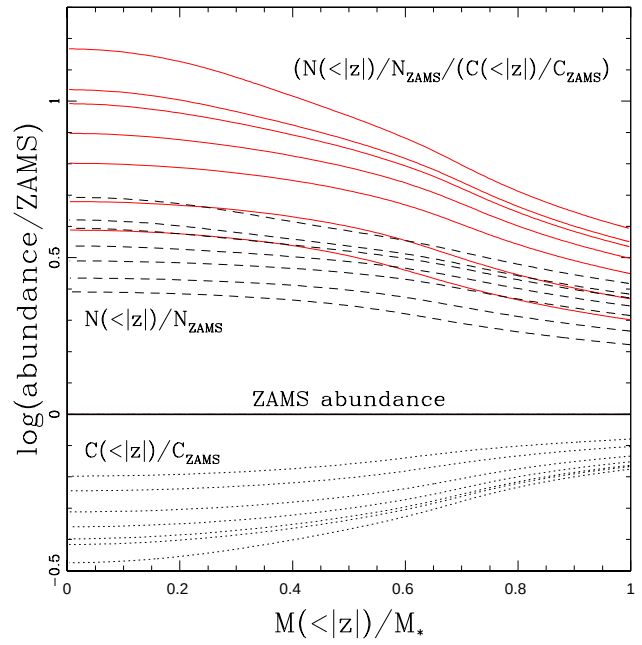



**Figure 6.** Enclosed carbon $C(<|a|)/C_{ZAMS}$ (black dotted), nitrogen $N(<|z|)/N_{ZAMS}$ (black dashed) abundances and their ratio (red solid), all measured relative to the initial ZAMS values, as a function of the enclosed mass fraction $M_*(<|z|)/M_*$ for the same times as in Figure 5. Already for the first profile distinguishable from the ZAMS abundances at 0.94 Gyr, the nitrogen to carbon ratio is enhanced by over a factor of three.

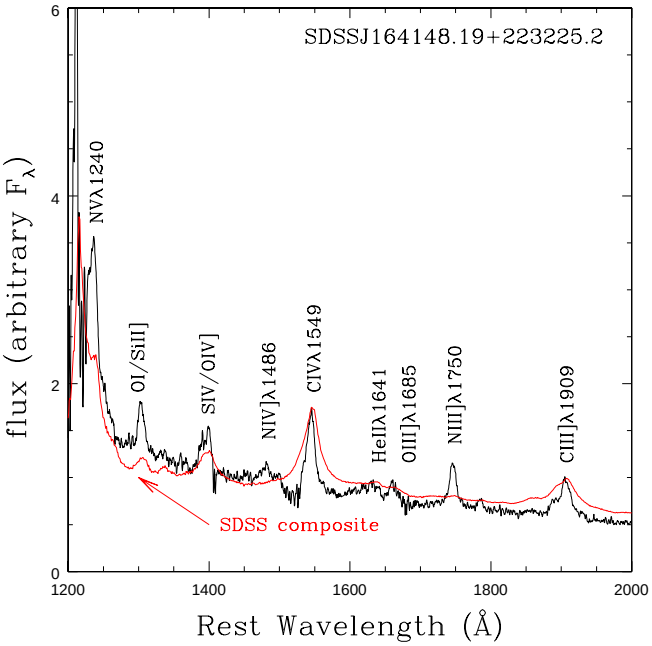



**Figure 7.** The spectrum of the nitrogen rich quasar SDSS J164148.19+223225.2 at $z = 2.51$ (black) identified by Batra & Baldwin (2014) in comparison to the SDSS composite quasar spectrum from Vanden Berk et al. (2001) in red.

with $z < 0$ is unbound. Hence, we next examine abundance anomalies as a function of $|z|$, To minimize the number of cases, we will just consider $M_* = 1M_\odot$. Higher mass stars show qualitatively similar properties, and lower mass stars are not very interesting because they have too little time to evolve.

Figure 5 shows the enclose helium mass faction, $Y(<|z|)$, as a function of the enclosed mass fraction $M(<|z|)/M_*$ over the course of a $M_* = 1M_\odot$ star's main sequence evolution. The helium abundance in the core steadily increases. While the average abundance grows by only $\simeq 35\%$ and the surface abundance is little changed, a significant fraction of the debris mass starts to be enhanced in helium by over 50% after the MS lifetime, and by over 100% at the end of the MS. Keep in mind that these central values are for slices through the star, so they are really averages of a slice through the core that is nearly 100% helium with a slice through the envelope that still has the initial helium abundance.

Figure 6 shows the changes in carbon, nitrogen and their ratio relative to their initial values as a function of the enclosed mass. Unlike the slow increase in the helium abundance, the initial depletion of carbon and enhancement of nitrogen is very rapid. Even by an age of $\sim 1$ Gyr, half the mass of the star has an average enhancement in $N/C$ of more than a factor of three. The rate of change then slows, but near the end of the star's MS lifetime, the average enhancement in the $N/C$ abundance ratio is roughly a factor of 10 for half the mass of the star.

The one potential problem with exploiting these abundance anomalies is that for a disruption at $R_p \simeq R_T$, the orbital time scales for debris produced by the core are long (years to decades), as also illustrated in Figure 5 based on Equation 1. The material accreted during the peak of the TDE light curve consist of material from the stellar surface layers with the initial ZAMS abundances. If having the processed debris material contribute to the emission lines requires that it complete an orbit and be processed through the resulting radiation-hydrodynamic complexities, then we must use disruptions at smaller pericentric radii, $R_p$. Since the characteristic orbital time scales shorten $\propto (R_p/R_t)^3$, only modest reductions in $R_p$ rapidly accelerate the evolution.

The second, and presently debated, possibility, is that photoionization of the debris stream contributes directly to the observed emission line spectrum. The fundamental issue is the solid angle subtended by the stream relative to the black hole, where the typical estimate for a normal quasar is that the broad line clouds have a covering fraction of order $f \simeq 10\%$ (e.g. Peterson 1997). The structure of the debris orbits leads to a roughly constant angular width in the orbital plane as seen from the black hole (see, e.g., Kochanek 1994). If the debris freely expands and maintains a roughly fixed spread in orbital inclination, then the debris stream can have a covering fraction of order a few percent and it will contribute significantly to the observed emission line spectrum, as in the models of Strubbe & Quataert (2009). If, on the other hand, the focusing effects of self-gravity and tides (see Kochanek 1994) lead to the vertical scale height expanding more slowly than the radius (roughly $r \sim t^{2/3}$), then the covering fraction of the debris stream is so small that it is probably unimportant to the observed spectrum, as in the models of Guillochon et al. (2014). An additional is-

sue is that the material with abundance anomalies will tend to lie at the stream center rather than the surface unless there is mixing. Since much of the stream is optically thick to photo-ionizing radiation (Kochanek 1994), emission lines generated by photoionizing the surface layers will show no evidence of the underlying abundance anomalies.

## 3 NITROGEN RICH QUASARS AND TDES

The nitrogen rich quasars are a rare spectral class, representing roughly 1% of SDSS quasars (Bentz & Osmer 2004, Bentz et al. 2004, Dhanda et al. 2007, Jiang et al. 2008). Jiang et al. (2008) argue that the nitrogen rich quasars are similar in redshift, luminosity, continuum slope, and black hole mass to most other quasars but have narrow carbon lines and a much higher radio loud fraction. Batra & Baldwin (2014) argue that the nitrogen rich quasars are biased to lower black hole masses, and that the strong nitrogen emission may require only high metallicity rather than nitrogen enhancement. It is difficult, however, to devise a stellar population that can produce enhanced nitrogen abundances unless the absolute metallicity is very high (see the discussion in Batra & Baldwin 2014). For illustration, Figure 7 shows the SDSS spectrum of the nitrogen rich quasar SDSS J164148.19+223225.2 identified by Batra & Baldwin (2014) in comparison to the SDSS composite quasar spectrum from Vanden Berk et al. (2001).

We instead propose that the nitrogen rich quasars are in fact TDEs. From §2, it is clear that TDEs provide a natural source of nitrogen-rich, carbon-poor material – the disruption of a single star easily provides sufficient mass to pollute the broad line region (BLR) of a quasar, since the mass in the BLR is only $\sim 10^{-3} M_\odot$ (e.g. Peterson 1997). The challenge is that, at least for Q0353−383, the anomalous spectra can persist for decades (Osmer 1980, Baldwin et al. 2003). The time scale problem from §2 is now reversed, in that we would now like longer orbital time scales than years to decades. This can be easily achieved if the disrupted star is a giant rather than a dwarf even for relatively low mass black holes ($10^6 M_\odot$, see, e.g., MacLeod et al. 2012), and then the time scale can be even longer of higher mass black holes.

However, as discussed in §2, disruptions of giants should be relatively rare, so for our proposal to be plausible, the rate required to explain the nitrogen rich quasars should be lower than the rate for all evolved stars. In Kochanek (2015), we estimate that the disruption rate of all evolved stars at $z \sim 2$ is $\sim 5\times10^{-9}$ Mpc$^{-3}$ year$^{-1}$. Batra & Baldwin (2014) found $N = 43$ nitrogen rich quasars in the redshift range $2.29 < z < 3.61$ from the 5740 deg$^2$ of SDSS DR5 (Adelman-McCarthy et al. 2007), corresponding to a survey volume of $V \simeq 89.4$ Gpc$^3$ ($\Omega = 0.3$, $\Lambda = 0.7$, $h = 0.7$). The mean redshift of the quasars is $\langle z \rangle = 2.80$. If the rest-frame lifetime of the event is $\Delta t = 10\Delta t_{10}$ years, then the required event rate is

$$r = \frac{N}{V(1+\langle Z\rangle)\Delta t} \simeq 1.3\Delta t_{10}^{-1} \times 10^{-11}\ \mathrm{Mpc}^{-3}\ \mathrm{year}^{-1}. \quad (2)$$

Alternatively, Jiang et al. (2008) identified $N = 293$ nitrogen rich quasars in DR5 with $1.7 < z < 4.0$, corresponding to a survey volume of $V \simeq 154$ Gpc$^3$, with $\langle z \rangle = 2.23$, yielding a comparable rate estimate of $r \simeq 5.9\Delta t_{10}^{-1} \times 10^{-11}$ Mpc$^{-3}$ year$^{-1}$. These are low enough compared to the estimated TDE rate for evolved stars in Kochanek (2015) that there seems no difficulty in creating the nitrogen rich quasars using the very long lived TDE's associated with the larger evolved stars.

A more general puzzle about abundances inferred from quasar BLRs is that they appear to require very high metallicities, $Z \gtrsim 5Z_\odot$ (e.g., Dietrich et al. 2003, Nagao et al. 2006). It is somewhat challenging to reach these metallicities with global star formation models (e.g., Hamann & Ferland 1993, Friaca & Terlevich 1998, Romano et al. 2002), leading to an alternative picture of star formation associated with the outer, self-gravitating parts of the accretion flow (e.g., Collin & Zahn 1999, Wang et al. 2011). BLR metallicity estimates use the steady increase of nitrogen relative to oxygen and carbon as the overall metallicity increases (Hamann & Ferland 1993). The N/C abundance ratios of $M_* \gtrsim M_\odot$ TDEs would naturally explain the observed abundance ratios without the need for stellar populations that are greatly super-Solar.

The challenge is producing enough disrupted mass to reasonably contaminate BLRs over long time scales. For quasars accreting near the Eddington limit, the accretion rate is of order $\dot{M}_E \simeq 0.2 M_{BH7} M_\odot$/year where the black hole mass is $M_{BH} = 10^7 M_{BH7} M_\odot$ and assuming a radiative efficiency of 10%. A rough estimate of the TDE rate for $M_* > M_\odot$ stars is $r \simeq 10^{-5}$/year below $M_{BH} \simeq 10^7 M_\odot$, dropping to $r \simeq 10^{-6.5}$/year at $M_{BH} \simeq 10^9 M_\odot$ (see Kochanek 2015). The drop at higher black hole masses is due to the increasing fraction of stars that pass through the event horizon without disrupting. Since the disrupted mass is of order $M_\odot$, the mass accretion rates supplied by TDEs, $\dot{M}_{TDE} \sim r M_\odot \sim 10^{-5} M_\odot$/year, are small compared to the average accretion rates of active black holes. This is simply a version of the point by Magorrian & Tremaine (1999) that TDEs cannot be a major component of quasar growth – it is feasible to temporarily contaminate the region around a quasar using TDEs as we propose for the nitrogen rich quasars, but is it not feasible to sustain the contamination in steady state.

The one interesting loophole is the observation by Arcavi et al. (2014) that a large fraction ($\sim 90\%$) of TDEs seem to be in post starburst galaxies, which otherwise represent only $\sim 1\%$ of galaxies (e.g., Quintero et al. 2004). Assuming post starburst galaxies represent recent mergers, and that mergers also are an important trigger of quasar activity (e.g. Hopkins et al. 2006), then the TDE rate when a quasar is active could be 100 times higher than when a quasar is inactive. Physically, the merger could temporarily lead to very rapid diffusion of stars into low angular momentum orbits or the presence of a binary black hole could greatly increase the rates (see, e.g., Li et al. 2015). This would still not compete with the overall accretion rate, but the overall rate at which TDEs would add mass to the region near the black hole, $\dot{M}_{TDE} \sim 10^2 r M_\odot \sim 10^{-3} M_\odot$/year, would no longer be negligible compared to the mass of the BLR.

## 4 DISCUSSION

A natural consequence of stellar evolution is that the debris in a TDE can show signs of nuclear processing. Be-

cause TDEs are likely dominated by lower mass stars ($M \lesssim 0.8M_{\odot}$) with very long evolutionary time scales, a large fraction should show no abundance anomalies. However, TDEs of more massive stars can have significantly enhanced helium and nitrogen abundances and depleted carbon abundances. The helium anomalies grow quasi-linearly with the elapsed fraction of the star's main sequence life time, while the carbon and nitrogen anomalies develop very quickly. We roughly estimate that $\sim 10\%$ of TDEs can show significant abundance anomalies. It is not feasible to predict how this might be modified by observational selection effects.

The average enhancement of helium is limited because it already represents a significant fraction of the stellar mass at birth, and helium is likely sequestered in the dense helium core once the star starts to ascend the giant branch. However, at fixed orbital period, debris including the core of a MS star can reach an average composition with roughly twice the initial helium mass fraction. Moreover, if the material at fixed period is not well-mixed, it actually consists partly of material with the initial helium abundance and partly of material that is almost entirely helium. Depending on the hydrodynamic evolution of the debris and the details of the geometry, the line emission observed by particular observers may be dominated by material with radically different local helium abundances even though the mean helium abundance is only modestly increased.

While not our focus, we should also note that TDEs occur at the centers of galaxies that typically contain stellar populations extending to higher metallicities than Solar. For example, our bulge contains stars of roughly twice Solar metallicity (e.g., Gonzalez et al. 2015), so $X = 0.64$, $Y = 0.32$ and $Z = 0.04$ for an initial number fraction of $f = n(He)/(n(H) + n(He)) = 0.11$ instead of $f = 0.09$. A 25% increase in the helium number fraction over Solar is neither huge nor negligible for addressing the line ratio problem discussed in §1. Furthermore, there are arguments that metal rich bulge stars are also helium enriched beyond this standard scaling (see, e.g., Nataf 2015). As discussed in §3, such super-Solar stars will also have larger ratios of $N/C$, although stars as metal rich as those invoked to explain quasar metallicities are very rare (or non-existent) in the Galactic bulge.

These TDEs should also show abundance anomalies in carbon, which is depleted, and nitrogen, which is enhanced. Oxygen also tends to be slightly depleted but by amounts that are probably unobservable. The changes in the carbon and nitrogen abundances occur very quickly, with the changes occurring in under 10% of the MS life time for the $M_* \gtrsim M_{\odot}$ stars that will show anomalies. Half the mass of a Sun-like star shows a change in the $N/C$ abundance ratio of over a factor of three almost immediately, growing to almost an order of magnitude by the main sequence turn off. More massive stars with stronger CNO cycles show still larger anomalies. However, the decline in both the IMF and stellar life times with stellar mass means that TDEs with carbon/nitrogen anomalies should almost all be $\sim 1M_{\odot}$ to $2M_{\odot}$ stars, almost independent of the assumed star formation history. Lower mass stars take too long to evolve, and higher mass stars are too rare.

For characterizing the abundance anomalies we used either the overall averages or averages at a fixed post-disruption period. For observational signatures, this may underestimate the importance of the processed material. As long as the disrupted material is not well-mixed, it will tend to have some memory of its initial density because its expansion and contraction will be roughly self-similar (e.g., Kochanek 1994). Thus, at fixed orbital period, higher density regions of the star will tend to be higher density regions of the debris. If the medium is optically thin and the density is low enough to avoid collisional de-excitation, then the strength of both recombination lines and collisionally excited lines are proportional to density squared rather than the linear weighting used in §2. This means that for debris with any "memory" of its initial density, our results in §2 could be underestimates of the observational effects of the abundance anomalies.

Considerable progress is being made in hydrodynamic simulations of TDES (e.g., MacLeod et al. 2012, Dai et al. 2013, Guillochon et al. 2014, Shiokawa et al. 2015, Bonnerot et al. 2016), although full radiation hydrodynamic simulations are needed given the likely importance of radiation to the flow properties (e.g., Loeb & Ulmer 1997, Strubbe & Quataert 2009, Miller 2015, Strubbe & Murray 2015, Metzger & Stone 2015). For probing the role of abundance anomalies, simulations need to track the distribution of debris as a function of abundance and/or initial radius within the star. First, this would address the question of mixing and residual correlations of abundance with density. Second, it would clarify the structure and thermal state of the debris streams. Third, for material that has returned to pericenter, it is important to determine if the debris ends up ordered inside out (i.e. long period material ends up at small radii due to hydrodynamics) or outside in (i.e. remains ordered by the post-disruption orbital binding energy).

For lower mass black holes, it is possible for a star to pass sufficiently close to the black hole to disrupt the far denser helium core of an evolved star. For simplicity we did not explore the details of such cases, since the event rate will be very low compared to the disruptions of main sequence stars or the envelopes of evolved stars. Obviously, such disruptions would allow still higher helium fractions and greater changes in CNO abundances. Anomalies in heavier elements, with the possible exception of s-process elements in the disruption of an AGB star, are unlikely to ever be observed because it requires the disruption of a rare massive star in the very (very!) short carbon burning phase.

A long standing puzzle in quasar spectra has been the small population ($\sim$ 1%) of nitrogen rich quasars (e.g. Bentz & Osmer 2004, Bentz et al. 2004, Dhanda et al. (2007), Jiang et al. 2008, Batra & Baldwin 2014). There are no natural mechanisms for evolving stellar populations to produce a nitrogen rich interstellar medium other than stellar populations with extremely high metallicities and even this may be problematic (see the discussion in Batra & Baldwin (2014)). TDEs can naturally supply a significant mass of nitrogen rich/carbon poor material, well in excess of the total mass required for a typical broad line region, and so could provide an explanation for the nitrogen rich quasars. Making the anomaly long lived (decades) would require the disruption of giant stars in order to have long time scales for the TDE, but the numbers of nitrogen rich quasars appear to be low enough to be compatible with the low rates of such events. This hypothesis does require, however, that the BLR emission of the nitrogen rich quasars

should evolve with time, so it would be interesting to survey the existing samples of nitrogen rich quasars for spectral changes.

It is difficult to use TDEs to explain the super-Solar metallicities estimated for quasars in general (e.g., Dietrich et al. (2003), Nagao et al. (2006)), basically because the average mass accretion rate from TDEs is small compared to the average accretion rate of black holes (Magorrian & Tremaine 1999). If, however, the observation by Arcavi et al. (2014) that a large fraction of TDEs are associated with post-starburst galaxies continues to hold, then the TDE rate during periods of quasar activity might also be enhanced by a factor of $\sim 10^2$. While still a small fraction of the mean accretion rate, the TDEs would supply a significant amount of material compared to that contained in the BLR.

The known TDEs are all at low redshift, where optical spectra will show signatures of anomalies in helium but not carbon and nitrogen. Searching for carbon and nitrogen anomalies requires ultraviolet spectra to probe the wavelength regions shown in Figure 7. This is feasible with the Hubble Space Telescope, and recent observations by Cenko et al. (2015) show that the TDE ASASSN-14li (Holoien et al. 2016) has a UV spectrum very similar to that of a nitrogen rich quasar, with strong NV, NIV] and NIII] lines and relatively weaker CIV and CIII] lines, as well as relatively strong HeII emission compared to normal quasars. This both bolsters our hypothesis for the origin of the nitrogen rich quasars and strongly suggests that ASASSN-14li was due to the disruption of a 1-2$M_\odot$ star. Because of the mapping between abundance and the original location of the material in the disrupted star, monitoring the evolution of such spectra should explore the evolving hydrodynamics of TDEs.

## ACKNOWLEDGMENTS

We thank R. Pogge for reminding us about the peculiar nitrogen rich quasars, J. Johnson, M. Pinsonneault and J. Tayar for answering many questions about stellar evolution and composition, T. Thompson for discussions and B. Shappee for comments. CSK is supported by NSF grants AST-1515876 and AST-1515927.

## REFERENCES

Adelman-McCarthy, J. K., Agüeros, M. A., Allam, S. S., et al. 2007, ApJS, 172, 634
Arcavi, I., Gal-Yam, A., Sullivan, M., et al. 2014, ApJ, 793, 38
Baldwin, J. A., Hamann, F., Korista, K. T., et al. 2003, ApJ, 583, 649
Batra, N. D., & Baldwin, J. A. 2014, MNRAS, 439, 771
Bentz, M. C., & Osmer, P. S. 2004, AJ, 127, 576
Bentz, M. C., Hall, P. B., & Osmer, P. S. 2004, AJ, 128, 561
Bonnerot, C., Rossi, E. M., Lodato, G., & Price, D. J. 2016, MNRAS, 455, 2253
Cenko, S. B., et al., 2015, http://astro-icore .phys .huji .ac.il/∼sites/∼astro-icore .phys .huji .ac.il/Sites/2015_Cenko_ApJ.pdf
Chornock, R., Berger, E., Gezari, S., et al. 2014, ApJ, 780, 44
Collin, S., & Zahn, J.-P. 1999, AAP, 344, 433
Dai, L., Escala, A., & Coppi, P. 2013, ApJL, 775, L9
Dhanda, N., Baldwin, J. A., Bentz, M. C., & Osmer, P. S. 2007, ApJ, 658, 804
Dietrich, M., Hamann, F., Shields, J. C., et al. 2003, ApJ, 589, 722
Evans, C. R., & Kochanek, C. S. 1989, ApJL, 346, L13
Friaca, A. C. S., & Terlevich, R. J. 1998, MNRAS, 298, 399
Gaskell, C. M., & Rojas Lobos, P. A. 2014, MNRAS, 438, L36
Gezari, S., Chornock, R., Rest, A., et al. 2012, Nature, 485, 217
Gonzalez, O. A., Zoccali, M., Vasquez, S., et al. 2015, arXiv:1508.02576
Guillochon, J., & Ramirez-Ruiz, E. 2013, ApJ, 767, 25
Guillochon, J., Manukian, H., & Ramirez-Ruiz, E. 2014, ApJ, 783, 23
Hamann, F., & Ferland, G. 1993, ApJ, 418, 11
Holoien, T. W.-S., Prieto, J. L., Bersier, D., et al. 2014, MNRAS, 445, 3263
Holoien, T. W.-S., Kochanek, C. S., Prieto, J. L., et al. 2016, MNRAS, 455, 2918
Hopkins, P. F., Hernquist, L., Cox, T. J., et al. 2006, ApJS, 163, 1
Jiang, L., Fan, X., & Vestergaard, M. 2008, ApJ, 679, 962
Kasliwal, M. M., Kulkarni, S. R., Quimby, R., et al. 2009, The Astronomer's Telegram, 2055, 1
Kochanek, C. S. 1994, ApJ, 422, 508
Kochanek, C. S. 2015, in preparation
Korista, K. T., & Goad, M. R. 2004, ApJ, 606, 749
Kroupa, P. 2001, MNRAS, 322, 231
Lacy, J. H., Townes, C. H., & Hollenbach, D. J. 1982, ApJ, 262, 120
Li, S., Liu, F. K., Berczik, P., & Spurzem, R. 2015, arXiv:1509.00158
Loeb, A., & Ulmer, A. 1997, ApJ, 489, 573
MacLeod, M., Guillochon, J., & Ramirez-Ruiz, E. 2012, ApJ, 757, 134
Magorrian, J., & Tremaine, S. 1999, MNRAS, 309, 447
Metzger, B. D., & Stone, N. C. 2015, arXiv:1506.03453
Miller, M. C. 2015, ApJ, 805, 83
Nagao, T., Maiolino, R., & Marconi, A. 2006, AAP, 447, 863
Nataf, D. M. 2015, arXiv:1509.00023
Osmer, P. S. 1980, ApJ, 237, 666
Paxton, B., Cantiello, M., Arras, P., et al. 2013, ApJS, 208, 4
Peterson, B. M. 1997, An introduction to active galactic nuclei, Publisher: Cambridge, New York Cambridge University Press, 1997 Physical description xvi, 238 p. ISBN 0521473489,
Quintero, A. D., Hogg, D. W., Blanton, M. R., et al. 2004, ApJ, 602, 190
Rees, M. J. 1988, Nature, 333, 523
Romano, D., Silva, L., Matteucci, F., & Danese, L. 2002, MNRAS, 334, 444
Roth, N., Kasen, D., Guillochon, J., & Ramirez-Ruiz, E. 2015, arXiv:1510.08454
Shiokawa, H., Krolik, J. H., Cheng, R. M., Piran, T., & Noble, S. C. 2015, ApJ, 804, 85

Strubbe, L. E., & Quataert, E. 2009, MNRAS, 400, 2070
Strubbe, L., & Murray, N., 2015, MNRAS in press [arXiv:1509.04277]
Vanden Berk, D. E., Richards, G. T., Bauer, A., et al. 2001, AJ, 122, 549
van Velzen, S., Farrar, G. R., Gezari, S., et al. 2011, ApJ, 741, 73
Wang, J., & Merritt, D. 2004, ApJ, 600, 149
Wang, J.-M., Ge, J.-Q., Hu, C., et al. 2011, ApJ, 739, 3
Wang, T.-G., Zhou, H.-Y., Komossa, S., et al. 2012, ApJ, 749, 115